New Phytologist

Research

Contrasting continental patterns of adaptive population divergence in the holarctic ectomycorrhizal fungus *Boletus edulis*

Keaton Tremble[1,2], J. I. Hoffman[3] and Bryn T. M. Dentinger[1,2]

[1]School of Biological Sciences, University of Utah, Salt Lake City, UT 84112, USA; [2]Natural History Museum of Utah, Salt Lake City, UT 84108, USA; [3]Department of Animal Behaviour, Bielefeld University, Bielefeld, 33501, Germany

Authors for correspondence:
Keaton Tremble
Email: keaton.tremble@utah.edu

Bryn T. M. Dentinger
Email: bdentinger@nhmu.utah.edu

Received: *15 July 2022*
Accepted: *26 September 2022*

New Phytologist (2023) **237:** 295–309
doi: 10.1111/nph.18521

Key words: *Boletus edulis*, ectomycorrhizae, fungi, local adaptation, population genomics, speciation.

Summary

- In the hyperdiverse fungi, the process of speciation is virtually unknown, including for the > 20 000 species of ectomycorrhizal mutualists. To understand this process, we investigated patterns of genome-wide differentiation in the ectomycorrhizal porcini mushroom, *Boletus edulis*, a globally distributed species complex with broad ecological amplitude.
- By whole-genome sequencing 160 individuals from across the Northern Hemisphere, we genotyped 792 923 single nucleotide polymorphisms to characterize patterns of genome-wide differentiation and to identify the adaptive processes shaping global population structure.
- We show that *B. edulis* exhibits contrasting patterns of genomic divergence between continents, with multiple lineages present across North America, while a single lineage dominates Europe. These geographical lineages are inferred to have diverged 1.62–2.66 million years ago, during a period of climatic upheaval and the onset of glaciation in the Pliocene–Pleistocene boundary. High levels of genomic differentiation were observed among lineages despite evidence of substantial and ongoing introgression. Genome scans, demographic inference, and ecological niche models suggest that genomic differentiation is maintained by environmental adaptation, not physical isolation.
- Our study uncovers striking patterns of genome-wide differentiation on a global scale and emphasizes the importance of local adaptation and ecologically mediated divergence, rather than prezygotic barriers such as allopatry or genomic incompatibility, in fungal population differentiation.

Introduction

Understanding the complex evolutionary pathways by which populations diverge and new species form has long been a goal of evolutionary biology (Fisher, 1930; Theodosius, 1982). Beyond gaining fundamental knowledge about the mechanisms that generate and maintain diversity, understanding the evolutionary history of genotypes and phenotypes allows us to predict how these characteristics will be impacted by environmental change. However, this understanding is challenging to achieve because the evolutionary processes that drive genetic divergence, such as demography, introgression, and adaptation, rarely act in isolation (Coyne *et al.*, 2004). Moreover, the dynamic interaction of these processes can produce differing signatures of divergence depending on the geographic and temporal scale of the study (Bierne *et al.*, 2013; Martin *et al.*, 2013; Peñalba *et al.*, 2019). To overcome the limitations of scale, and disentangle the complex evolutionary web weaved by the speciation process, research must be conducted within a global context.

Tractable systems that exhibit dynamic properties for which hypotheses can be generated and tested are essential to studying processes that give rise to genetic divergence in wild organisms. Species that are common, widely distributed geographically and ecologically, and highly variable are ideal targets for determining the genetic basis of divergence (Hoban *et al.*, 2016). For example, systems such as the monkey flowers (*Mimulus* spp.) (Ferris *et al.*, 2017; Puzey *et al.*, 2017; Vallejo-Marín *et al.*, 2021), black cottonwood (*Populus trichocarpa*) (Evans *et al.*, 2014; Geraldes *et al.*, 2014; McKown *et al.*, 2014), and three-spine stickleback (*Gasterosteus aculeatus*) (Hohenlohe *et al.*, 2010; Feulner *et al.*, 2015; Marques *et al.*, 2018) have been used to investigate how the complex interaction of demography, introgression, and local adaptation gives rise to genetic variation and population differentiation during speciation. However, none of these systems exhibit a truly global distribution or continuous ecological breadth, limiting our ability to investigate the interaction of evolutionary processes unconstrained by geography or ecology. Moreover, these examples give insight into processes in only a few plants and animals, limiting the generality of the observations. The third major eukaryotic lineage, *Fungi*, remains critically understudied (Coyne *et al.*, 2004; Giraud *et al.*, 2008; Gladieux *et al.*, 2014) despite its ecological importance, enormous diversity, and more tractable genomes. The globally distributed prized edible 'porcini' mushroom, *Boletus edulis*, fulfills

the need to study processes that both give rise to genome-wide divergence at a global scale and include organisms other than plants and animals.

Boletus edulis Bull. ('porcini') is a well-known ectomycorrhizal species complex that is found in nearly all temperate ecosystems across the northern hemisphere (Smith, 2005). Due to extensive phenotypic variation (Fig. 1), the taxonomy of *B. edulis* is a matter of some controversy with many alternative classifications (Arora, 2008; Dentinger *et al.*, 2010; Arora & Frank, 2014). Current molecular evidence is equally ambiguous, indicating that this complex group may be in the early stages of speciation (Coyne *et al.*, 2004; Beugelsdijk *et al.*, 2008; Dentinger *et al.*, 2010; Tremble *et al.*, 2020). Taken together, the combination of morphological variation, enormous ecological amplitude, holarctic distribution, and small genome (*c.* 50 Mbp) makes *B. edulis* an ideal natural system to investigate the roles of demography, introgression, adaptation, and isolation in the speciation process at a global scale. Here, we utilize population genomics, ecological niche, and demographic modeling to investigate the primary forces driving lineage divergence within *B. edulis* and to identify loci under putative selection within a global and historical context.

Materials and Methods

Characterizing population structure in *B. edulis*

An investigation of the processes that facilitate population differentiation relies on a thorough understanding of the demographic history and distribution of diversity within the focal group. Previous attempts to characterize population genetic structure within *Boletus edulis* Bull. have been inconclusive (Tremble *et al.*, 2020). Therefore, we first used a coalescent-based phylogenomic approach to segregate *B. edulis* specimens into lineages. Then, we characterized the geographical distributions and genomic diversity of these lineages. One hundred and sixty *B. edulis* specimens were gathered from a global distribution using a combination of targeted field collection and institutional loans from fungaria in North America (102 specimens), Asia (10 specimens), and Europe (51 specimens) (Supporting Information Table S1). No specimens collected before 1950 were analyzed in order to maximize DNA library integrity and to minimize any possible effects of time on our results. Specimens of *B. reticuloceps*, *B. variipes*, and *B. barowsii* were included as out-groups (Dentinger *et al.*, 2010).

Genomic DNA was extracted from 10 mg of hymenophore tissue using the Monarch® Genomic DNA Purification Kit (TS3010). DNA extracts were assessed for quality using a NanoDrop 1000 spectrophotometer (Thermo Scientific) and for integrity using agarose gel electrophoresis. Sequencing was performed using a combination of paired-end sequencing on the Illumina MiSeq, HiSeq, and Novaseq platforms (Table S2). Raw reads were quality-filtered and adapter-trimmed using fastP v.0.20.1 (Chen *et al.*, 2018) with default settings. Genome assemblies were generated from quality-filtered reads using SPAdes v.3.15.0 (Bankevich *et al.*, 2012) with five *k*-mer values ($k = 77$, 85, 99, 111 and 127) to maximize assembly quality. The publicly available assembly of *Paxillus involutus* (Kohler *et al.*, 2015) was used as the out-group. Exonerate v.2.2.0 (Slater & Birney, 2005) was used to extract 702 single-copy orthologs conserved across the Boletales identified by the Boletales MCL clustering in Mycocosm (Grigoriev *et al.*, 2014). Retained orthologs were aligned using Mafft v.7.397 (Katoh *et al.*, 2017) with the L-INS-i algorithm, and maximum-likelihood gene trees were produced using Iq-tree v.2.0.3 (Minh *et al.*, 2020) with automatic model selection in ModelFinder (Kalyaanamoorthy *et al.*, 2017) and 1000 ultrafast bootstrap (Hoang *et al.*, 2018) replicates. Branches with poor support (BS ≤ 10%) were removed before generating a summary coalescent species tree using Astral-III v.5.7.5 (C. Zhang *et al.*, 2018). The '*Boletus edulis*' group was defined as the monophyletic group sharing a most recent common ancestor with *B. reticuloceps*. All specimens that fell outside of the *B. edulis* and *B. reticuloceps* groups were reclassified as 'non-edulis', and geographically monophyletic genetic clusters within *B. edulis* were identified as distinct lineages.

To characterize patterns of admixture and haplotype diversity across the landscape, we used the highly contiguous *B. edulis* assembly (Tremble *et al.*, 2020). For improved gene prediction, total RNA was extracted from frozen hymenophore tissue of sample BD747 (Tremble *et al.*, 2020) using TRI Reagent® (Sigma-Aldrich) following the manufacturer's instructions. Short-read mRNA enrichment, library prep, and paired-end sequencing were performed by Novogene USA (Sacramento, CA, USA). Full-length cDNA was sequenced on a single Oxford Nanopore Technologies (Oxford, UK) R9.4 flow cell in a MinION device after mRNA enrichment and library preparation using a Direct cDNA Sequencing Kit (SQK-DCS109) following the manufacturer's protocols. The Funannotate v.1.8.6 (Palmer, 2022) genome annotation wrapper script was used for gene prediction according to best practices. In brief, short-read DNA/RNA and

Fig. 1 Examples of phenotypic variation across the global distribution of *Boletus edulis*. Numerous attempts have been made to segregate groups of *B. edulis* into new species based on this phenotypic variation, yet these attempts have not been corroborated by genetic evidence.

long-read cDNA were used to first create a PASA training model, which was utilized to guide Augustus (Hoff & Stanke, 2018) gene prediction with assembled mRNA transcript evidence. Functional annotation of predicted genes utilized InterProScan5 (Jones *et al.*, 2014), Eggnog-Mapper v.2.0.8 (Cantalapiedra *et al.*, 2021), dbCan2 (H. Zhang *et al.*, 2018), SignalP v.5.0 (Almagro Armenteros *et al.*, 2019), and antiSmash v.6 (Medema *et al.*, 2011).

To identify genome-wide single nucleotide polymorphisms (SNPs), we mapped adapter-trimmed and quality-filtered reads to our reference using Bowtie2 v.2.2.6 (Langmead & Salzberg, 2012). SNP genotyping was performed with Gatk v.4.20 using their best practices for nonmodel organisms (Kryvokhyza, 2021). To retain only high-confidence variants, we removed putative SNPs with > 5% missing data, fewer than two alleles, and a min/max mean read depth below 10 and above 75 with VCFtools v.0.1.15 (Danecek *et al.*, 2011). We then removed any specimen with > 30% missing data to prevent spurious population assignments due to limited information. Some analyses such as principle component analysis (PCA) and admixture analysis require independent observations. Therefore, we used Plink v.1.9 (Purcell *et al.*, 2007) to prune out SNPs in high linkage disequilibrium (LD) ($r^2 > 0.2$, 50 kbp windows, 10 bp step) to create a secondary LD-pruned dataset. To identify the overlap between phylogenomic lineages and population structure, we performed PCA with our LD-pruned dataset using the R package adegenet v.2.1.3 (Jombart, 2008). To identify patterns of shared ancestry, we conducted an admixture analysis per specimen. Briefly, admixture analyses identify the proportion of SNPs within the genome that correspond to one of *X* number of ancestral populations (termed '*K*'). Ancestry admixture analysis was performed with the snmf function of the R package lea v.3.2.0 (Frichot *et al.*, 2014) on the LD-pruned dataset using sites with no missing values, with 10 runs each for *K* values between 4 and 8. The run with the lowest cross-entropy for each *K* was selected for the final admixture assessment. For a detailed flowchart of population genomic methods and SNP datasets used for each analysis, see Fig. S1.

Characterizing the geographic structure of widely dispersed lineages

To characterize population structure, and to test for population substructure within *B. edulis* lineages, we conducted a two-part analysis. First, using our LD-pruned dataset, we performed PCA and produced neighbor-joining trees for each lineage with the R package adegenet v.2.1.3 and identified whether significant clusters were present irrespective of geography. Second, to identify whether genetic distance (relatedness) between any two specimens significantly correlates with geographic distance (suggesting isolation by distance: IBD) or environmental distance (suggesting isolation by environment: IBE), we used a multiple matrix regression approach (Wang, 2013) to assess the correlation between geographic, environmental, and genetic distance matrices as well as the interaction between geographic and environmental distance. Euclidean geographic distances were calculated using GPS coordinates and the dist() function of base R and log transformation. To capture environmental metrics for each specimen, we utilized the Bioclim dataset (Fick & Hijmans, 2017). The 19 Bioclim variables for each individual were extracted at a 30-s scale using the R package gdalutils (O'Brien, 2022) and plotted using PCA. Then, Euclidean geographic distances between individuals on the PCA were calculated using the pca2dist function of the R package ape (Paradis *et al.*, 2004) and stored as an environmental distance matrix. We used two methods to calculate genetic distances as each may produce separate measures of relatedness: absolute pairwise genetic distances using the dist.gene function in ape; and, first using PCA clustering and then calculating Euclidean distances between individuals. Both measures were calculated using our LD-pruned SNP dataset.

Identification of interlineage introgression and genome-wide diversity and divergence

To determine the extent of divergence, and whether this divergence indicates a pervasive lack of gene flow, we used a Bayesian coalescent approach to estimate the divergence dates of lineages, calculated the magnitude and genomic distribution of divergence and diversity, and determined whether significant signatures of introgression between lineages were present. To date the divergence of the *B. edulis* lineages, we used the multiple-species-coalescent model within the Bayesian platform StarBeast2 (Ogilvie *et al.*, 2017) using an estimated 100 million years ago (Ma) (95% CI = 70–150 Ma) divergence date for the *Boletaceae* (He *et al.*, 2019). Due to computational limitations of Beast2, a reduced representation matrix was used, composed of two randomly selected, but geographically distinct, representatives from each *B. edulis* lineage, with *B. reticuloceps*, *B. variipes*, and *P. involutus* as out-groups. Twenty of the 702 single-copy genes were randomly selected, and putative orthologs of these genes in each genome were aligned in Mafft, as mentioned in the previous section. Best-clock models were automatically chosen with bModelTest (Bouckaert & Drummond, 2017), site models were set to all-reversible, and an *a priori* initial clock rate of 0.001 was chosen based on estimated mutation rates in related taxa (Chen *et al.*, 2015). The MCMC chain was run for 10^7 cycles, and all parameters reached acceptable convergence based on ESS values > 200. The final tree was produced using Tree-Annotator with an empirically determined burn-in (10%).

To estimate the degree of genomic divergence, we calculated F_{ST}, a measure of shared and fixed alleles between two populations. We also calculated absolute divergence $D_{(xy)}$, a metric that is robust to variation in within-population nucleotide diversity (Nei, 1987). Pairwise F_{ST} and $D_{(xy)}$ were calculated across 10 kb nonoverlapping windows using the program Pixy (v.1.2.2) (Korunes & Samuk, 2021), which facilitates the use of invariant sites to compensate for missing data, critical for accurate assessments of $D_{(xy)}$. Nucleotide diversity across synonymous and nonsynonymous sites was calculated across all genes on scaffold 1 using the program SNPGenie (Nelson *et al.*, 2015). Population summary statistics for each lineage were calculated using the non-LD-pruned dataset in the R package PopGenome v.2.7.5 (Pfeifer *et al.*, 2014) across the top 100 largest genomic scaffolds. To

determine whether differentiation was limited to noncoding regions, we limited our dataset to include only genic regions and identified the number of highly differentiated genes for each population (F_{ST} vs all > 0.75). Lastly, to identify significant signatures of introgression and to verify the presence of gene flow between lineages, we calculated Patterson's *D* statistic (ABBA–BABA) using the DSUITE command line package (Malinsky *et al.*, 2021) on all phylogeny-compatible quartets. Patterson's *D* is a robust and widely used approach to identify patterns of shared inheritance between diverged groups while accounting for confounding demographic processes such as incomplete lineage sorting (Zheng & Janke, 2018).

Identifying the genetic basis of local adaptation

We used a two-part analysis to identify highly divergent loci with predicted molecular function that also possessed significant signatures of local adaptation. First, we calculated pairwise F_{ST} and $D_{(xy)}$ statistics with PIXY using only genic regions in our all-sites filtered dataset (Fig. S1). We then calculated the average pairwise F_{ST} and $D_{(xy)}$ for each gene and for each lineage. Our final dataset of highly divergent loci included genes that were in the top 5% of both F_{ST} and $D_{(xy)}$. To prevent the spurious retention of loci that have diverged due to genetic drift and not divergent selection, we used the program PCADAPT (Luu *et al.*, 2017). PCADAPT utilizes PCA to account for demographic structure and identifies SNPs with signatures of local adaptation (patterns of fixation that may be indicative of local adaptation) in excess of what would be expected from drift alone. A *K* value of 3 was used as this represented the first plateau identified in a scree plot (Fig. S2), and Bonferroni correction (alpha = 0.01) was performed to produce a high-confidence dataset. To combine our analyses, we reduced our dataset of highly divergent top 5% F_{ST} and $D_{(xy)}$ loci to only those genes that contained SNPs with significant signatures of local adaptation ($P < 0.05$), as determined through PCADAPT.

Identifying climatic partitioning

We utilized an ecological niche modeling approach to predict the probability of persistence across the landscape based on environmental suitability. Specifically, to identify whether current distributions of *B. edulis* populations represent distinct ecological niches, we used MAXENT v.3.4.1 (Elith *et al.*, 2011) to model the potential niche distribution likelihoods of all lineages based on environmental conditions as determined by the 19 Bioclim variables. Default settings were used with 100 replicates. Model fit was assessed with the popular 'area under the receiver-operator curve' (AUC) metric (Merow *et al.*, 2013), and the contribution of each climatic variable was calculated using jackknife contributions to AUC.

Demographic and paleo-climatic niche modeling to identify correlations between isolation and genome-wide divergence

Interpreting the evolutionary history of a taxon from contemporary distribution patterns is complicated by numerous evolutionary pathways that can lead to strikingly similar results. For example, strong geographic population structure can be the product of selection for regional environmental conditions, or from periods of isolation in refugia during Pleistocene glaciation. In order to identify whether divergence in *B. edulis* is mediated by ecological adaptation in the face of gene flow, or by periods of allopatric isolation and drift, we utilized a two-part analysis that modeled rates of gene flow between pairs of lineages and then determined whether geographic connectivity between lineages was broken during glaciation by unsuitable habitat. First, we simulated five different two-population demographic scenarios (Fig. 5, see later) and compared these models to two empirical datasets of sister lineages: West coast/Colorado and Alaska/East coast. Our specific models were isolation without migration, ancient gene flow followed by isolation, isolation followed by recent gene flow (secondary contact), continuous gene flow after divergence, and differential gene flow as reproductive barriers form (high then low). Empirical datasets consisted of 2-D unfolded site frequency spectra between each lineage pair produced using easySFS and our LD-pruned SNP dataset to include only independent markers (Overcast, 2022). Models were implemented using FASTSIMCOAL2 v.2.6.0.3 (Excoffier *et al.*, 2021). Each model was run for 200 000 simulations across 50 iterations and rerun 100 times. We used the Akaike information criterion to determine the best run for each model. To find the best model for each pair of sister taxa, we reran each initial model 100 times using the parameters determined within the best run and compared the distribution of likelihoods between all five models. To corroborate these demographic models in a separate analysis, we used ecological niche modeling to determine whether each pair of sister lineages likely maintained constant geographic contact, or were geographically isolated during cycles of glaciation. Specifically, we reran our previous ecological niche modeling analysis on a second dataset of the 19 Bioclim variables produced from models of environmental conditions during the last glacial maximum approximately 22 000 years ago.

Results and Discussion

Characterizing population structure in the globally distributed *B. edulis*

To investigate the demographic history of a globally distributed taxon and to elucidate population differentiation, we sequenced whole genomes from 161 specimens of *B. edulis* and three outgroup species. We first generated a high-quality reference genome from a North American *B. edulis* specimen (N50 = 149 kb; 16 573 protein-coding regions; 97.3% BUSCO completeness) and re-sequenced 160 *B. edulis* specimens from across its global distribution, with three additional members of 'porcini' *sensu stricto* (Dentinger *et al.*, 2010). Coalescent phylogenomic reconstruction of 702 single-copy genes revealed a monophyletic *B. edulis* composed of six clades that share a most recent common ancestor with the Asian endemic *B. reticuloceps* (Wang & Yao, 2005) (Fig. 2a). Five of the six nodes had 100% support, and the sixth received full support in a separate concatenated supermatrix

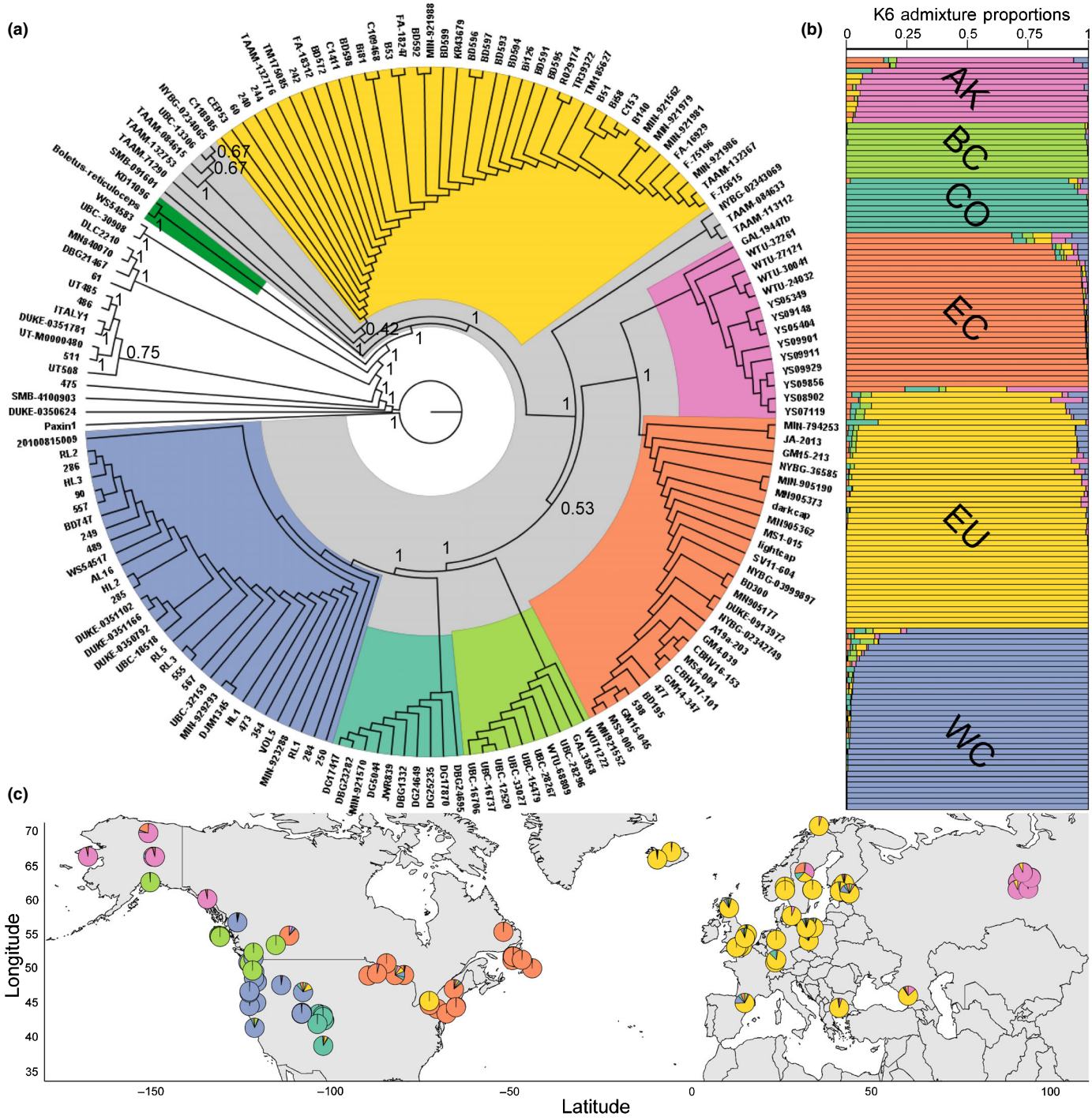

Fig. 2 Population structure analysis of *Boletus edulis*. (a) Coalescent phylogenomic reconstruction of the group from 702 single-copy gene trees. *B. edulis* (highlighted in gray) is defined here as all individuals sister to *Boletus reticuloceps* (highlighted in dark green). Colors indicate geographically structured clades; *B. edulis* individuals not in groups are ambiguously placed predominately due to poor genome assembly and low recovery of signal copy genes. Values at nodes indicate nodal quartet support. (b) LEA admixture analysis assuming six ancestral populations (*K*6) from 52 112 high-confidence, linkage disequilibrium-pruned variants. Bar height and color indicate the proportion of genome-wide single nucleotide polymorphisms (SNPs) within each individual that correspond to each putative ancestral population (AK, Alaska/Russia; BC, British Columbia; CO, Colorado; EC, east coast North America; EU, Europe; WC, west coast North America), and (c) the distribution of admixture results from plot B across the range of *B. edulis*.

analysis that recovered the same topology (Fig. S3). Thirteen specimens were assigned to other species, illustrating the extent to which taxonomic uncertainty of *B. edulis* can compromise reliable identification on the basis of morphology alone. To prevent the inclusion of misidentified specimens in subsequent analyses, we retained only individuals that were clustered within these six *B. edulis* lineages (147 of 160 initial specimens). These groups are strongly geographically structured and are hereafter referred

to as Europe (EU), Russia/Alaska (AK), North America east of the Rocky Mountains (EC), British Columbia (BC), Colorado (CO), and North America west of the Rock Mountains (WC) lineages. Importantly, the boundaries of these lineages do not directly correspond with previously recognized morphotaxa. For example, the WC lineage is comprised of both the previously segregated morphotaxon *B. edulis* var. *grandedulis* from California as well as specimens not previously differentiated from Utah, Washington, Oregon, and British Columbia. This conflict highlights the phenotypic diversity within *B. edulis* and suggests a disconnect between phenotypic similarity and genetic relatedness.

To determine the magnitude and spatial distribution of admixture among the six lineages of *B. edulis*, we identified 792 923 high-confidence genome-wide variants from 137 individuals that remained after quality filtering. The six lineages were recovered in both admixture ($K = 6$) (Fig. 2b,c) and PCA analysis (Fig. S4), further indicating a strong phylogeographic structure. The extent of admixture varied widely between lineages (mean admixture AK = 8.7%, BC = 0.6%, CO = 2.0%, EC = 5.9%, EU = 6.5%, WC = 3.4%). However, four out of the six lineages (AK, EC, EU, and WC) contained at least one individual exhibiting > 30% mixed ancestry, suggesting a recent history of migration. Surprisingly, we identified contrasting patterns of admixture between geographically adjacent lineages. Asian individuals within the AK lineage exhibit a moderate signature of shared ancestry with EU, yet North American individuals within the same lineage exhibit admixture predominately with the EC group. In addition, lower values of K (putative ancestral populations) collapse the AK lineage into hybrids of EC and EU, further indicating a history of migration between AK and the EC and EU lineages (Fig. S5). By contrast, the WC lineage has more admixed ancestry with the EU lineage than either BC or CO despite geographic and phylogenetic proximity. Interestingly, one individual collected in North America carries a EU genotype, with little admixture (Fig. 2c). This specimen was collected in a monodominant stand of Norway spruce *Picea abies*, a tree species native to Europe that is commonly introduced in North America (Klimo *et al.*, 2000). This strongly suggests that this individual represents a recent anthropogenic introduction, so we removed it from further analyses. Altogether, admixture analysis of *B. edulis* indicates that admixture is lineage- and context-specific and that geographic proximity appears to predict admixture for some lineages, while other groups experience minimal admixture with parapatric neighbors.

Characterizing the geographic structure of widely dispersed lineages in *B. edulis*

Within-lineage PCA (Fig. S6 left) and neighbor-joining trees (Fig. S6 right) show no clear patterns of within-lineage geographic clustering for all five of the lineages except AK. The AK lineage exhibits clear geographic structure, comprised of three genetically distinct groups corresponding to Western Russia and two within Alaska. To corroborate these findings, we used multiple matrix regression (Wang, 2013) to empirically test for isolation by distance (IBD) and isolation by environment (IBE) and found that IBD was not significant ($P > 0.05$) for all lineages except AK ($P < 0.05$), and IBE was only significant for the WC population. Given the very large spatial distribution of the AK lineage and our patchy sampling, this signature of IBD is unsurprising. However, it is striking that the EU lineage, which persists across the entirety of Europe, including westward to Iceland and eastward to Georgia, does not show any signatures of population substructure. Most, if not all, systems previously utilized for large-scale population genomic analysis exhibit some degree of IBD, particularly at the regional to continental scale. For example, studies of both *Populus trichocarpa* and *Mimulus guttatus* found limited IBD at local scales, but strong IBD at regional scales suggesting dispersal limitation across landscapes (Geraldes *et al.*, 2014; Twyford *et al.*, 2020). It is possible that the lack of IBD in the EU lineage is a product of cryptic environmental adaptation of widely dispersed and divergent environments (Jiang *et al.*, 2019). However, the multiple matrix regression method used here empirically tests for the association of genetic distance and the interaction of geographic distance and environmental distance, while controlling for IBE in the assessment of IBD. In addition, given the prominent commercial trade of *B. edulis* in Europe, it is possible that the lack of IBD identified within the EU lineage could be due to anthropogenic mediated dispersal. While this possibility is difficult to account for in our analyses, if anthropogenic dispersal was the primary force responsible for the lack of geographic structure in the EU lineage, we would expect to have identified a contrary pattern in North America *B. edulis*, where there is limited commercial sale of *B. edulis* (Dentinger & Suz, 2014; Ii *et al.*, 2021). However, we have identified no signature of IBD in the lineages of North America, suggesting that anthropogenic dispersal does not significantly erode population structure. Moreover, the commercial trade of *B. edulis* is often local in scale, and approximately 50% of the European 'porcini' trade consists of imported *Boletus* species from China that are not *B. edulis* (Sitta & Floriani, 2008; Dentinger & Suz, 2014). Lastly, the practice of planting non-native trees in managed plantations for timber production is common in Europe and may be another factor contributing to the lack of IBD found in the EU lineage (Siry *et al.*, 2005). The forests of Iceland are an extreme example of this practice; *Betlua*, *Salix*, and sparse *Populus* are the only native ECM host genera on the island and the commonly found Norway spruce *Picea abies* is introduced (Bragason, 1995). The EU specimens from Iceland were collected under Norway spruce and thus may have been introduced. However, we found no significant correlation between genetic distance and geographic distance ($P = 0.143$) after removing the Icelandic samples, suggesting that the lack of IBD in the EU lineage is not solely due to the introduction of potential non-native hosts. On a continental scale, we found contrasting signatures of population structure between North America and Europe. In Europe, there is a single widely distributed lineage, yet in North America, there is strong geographic separation of five lineages. Differences in phylogeographic or population structure between closely related groups have been identified in other systems (Hickey *et al.*, 2009) and are often associated with differences in dispersal capacity. However, to the best of our knowledge, no other system exhibits such contrasting signals of geographic structure between

continents. Differences in dispersal capacity could potentially produce similar patterns of contrasting geographic structure (Bohonak, 1999), yet only the widely distributed and sparsely sampled AK lineage exhibited any degree of IBD or subpopulation structure. This suggests that the dispersal capacity of these populations may exceed far beyond their current (in some cases narrow – BC and CO) range distributions, which may be indicative of local environmental adaptation.

Identification of interlineage introgression and genome-wide diversity and divergence

To understand the evolutionary history of divergence in *B. edulis*, we performed phylogenetic divergence dating using StarBEAST2 and the multiple-species coalescent using a 100 Ma most recent common ancestor (MRCA) (He *et al.*, 2019) of the *Boletaceae* and found a surprisingly ancient split between extant lineages. The MRCA of *B. edulis* was dated to 2.66 Ma (2.14–3.17 95% HPD, Fig. S7) and the most recent split, between AK and EC lineages, to 1.52 Ma (0.72–2.35 95% HPD) (Fig. 3c). The exact timing of divergence identified here should be viewed as an approximation, as the lack of a fossil record prevents more accurate estimates. However, a root age of 2.66 Ma corresponds with a period of well-documented climatic upheaval and onset of glaciation during the Pliocene–Pleistocene boundary, which is known to have spurred divergence in other groups, providing support for our estimate (Ericson *et al.*, 1963; Shackleton & Opdyke, 1977; deMenocal, 2004). The subsequent rapid three-way separation of Europe from the two North American/Asian groups is suggestive of a single widely distributed ancestral lineage that split geographically, a similar pattern to that found in the *Picea likiangensis* species complex at the Pliocene–Pleistocene boundary (Sun *et al.*, 2018).

Pairwise population differentiation F_{ST} and divergence $D_{(xy)}$ analyses revealed moderate-to-strong genome-wide differentiation (Figs 3a, S8 bottom, Table S2) in *B. edulis*. Most lineage pairs possessed F_{ST} and $D_{(xy)}$ values (total F_{ST} mean across 10 kb windows = 0.471, $D_{(xy)}$ = 0.128) as large or larger than values

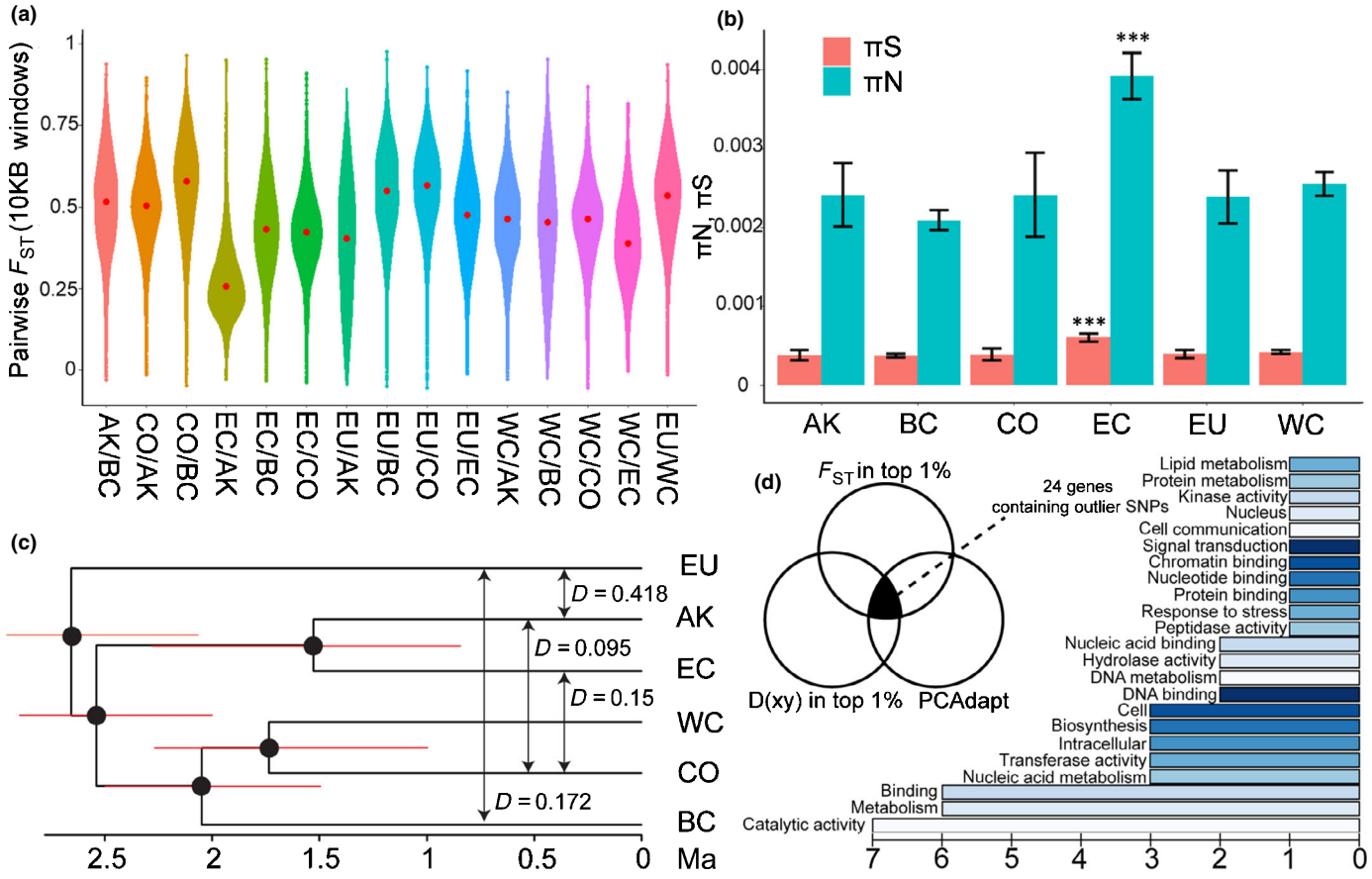

Fig. 3 Population genomic analysis of *Boletus edulis* population differentiation, divergence, and introgression. (a) Pairwise F_{ST} values calculated across 10 kb windows. Red points indicate median value, (b) per site nucleotide diversity π calculated at nonsynonymous and synonymous sites for all genic regions on the 1.6 Mbp scaffold 1, error bars represent SD, '***' indicates significant differences ($P < 0.001$ ANOVA), (c) divergence time estimation of *B. edulis* populations utilizing StarBEAST2 and all significant results of ABBA-BABBA introgression analysis. Horizontal red bars represent 95% confidence range of node divergence date and vertical black arrows with corresponding *D* statistic between specific population pairs. (d) Outlier analysis of potentially adaptive loci. Outlier genes were identified as loci in the 99th percentile of mean pairwise F_{ST} and $D_{(xy)}$ that contained a significant ($P < 0.05$) putative locally adapted loci identified by PCAdapt (left). All potential Gene Ontology (GO) terms for the 24 outlier genes were placed into categories by SlimGo (right). The number of genes within each category is indicated by values along the *x*-axis, and bar colors are randomly generated for ease of viewing. AK, Alaska/Russia; BC, British Columbia; CO, Colorado; EC, east coast North America; EU, Europe; WC, west coast North America.

commonly found in groups of well-differentiated taxa (Martin *et al.*, 2013; Klimova *et al.*, 2017; Rovito & Schoville, 2017; Zhong *et al.*, 2019). Furthermore, there was no significant difference between F_{ST} and $D_{(xy)}$ values calculated across 10 kb windows and genes, indicating that divergence is genome-wide and not limited to regions with low selective constraint. In contrast to all other lineage pairs, AK/EC exhibited significantly lower F_{ST} (mean = 0.2739, $P < 0.0001$), which is well within the expected range for populations experiencing ongoing gene flow (Callahan *et al.*, 2013; Branco *et al.*, 2017; Garcia-Elfring *et al.*, 2017), and exhibited a skewed distribution of F_{ST} values with an excess of highly diverged loci (Fig. S9). Visualizing the distribution of F_{ST} values across the genome can provide insights into the strength of homogenizing gene flow between populations (Seehausen *et al.*, 2014). Allopatric populations generally exhibit values of divergence that are normally distributed around a global mean with a greater-than-expected abundance of conserved housekeeping loci. By contrast, parapatric populations typically exhibit skewed distributions, with most of the genome exhibiting low divergence due to homogenization by gene flow, and an excess of highly diverged regions around barrier loci (Nosil *et al.*, 2012; Martin *et al.*, 2013). *QQ* plots show that only AK/EC exhibits a skewed F_{ST} distribution, indicating that most lineages of *B. edulis* have high genomic divergence that is not being eroded by gene flow.

The EC lineage exhibited significantly higher nucleotide diversity (π) across both nonsynonymous and synonymous positions, while there were no significant differences among any of the other lineages. The substantially increased diversity within the EC lineage in combination with a skewed distribution of F_{ST} values (Fig. S9) provides strong evidence for ongoing gene flow, predominately from AK into EC. The similar levels of diversity of all of the other lineages are surprising given the differences in the geographic ranges of these groups. For example, the CO lineage is distributed across a subset of the American Southwest, a fragmented landscape of habitat islands surrounded by desert basins, but had similar nucleotide diversity (π) to the EU lineage, which has a continent-wide distribution. Landscape fragmentation is often found to be negatively associated with nucleotide diversity (Gaines *et al.*, 1997; Dixo *et al.*, 2009), in contrast to our results. This may be explained by a recent rapid expansion of the EU lineage, which is suggested by a highly negative genome-wide Tajima's *D* (mean = −1.149, Fig. S8 top). Alternatively, or in addition, these patterns might be explained by high dispersal capacity regardless of range size or landscape fragmentation.

Ancient divergence, high genomic differentiation, and low levels of admixture strongly suggest that lineages of *B. edulis* are well segregated. To empirically test for signatures of introgression and gene flow, we calculated the four-population ABBA–BABA (Patterson's *D*) (Malinsky *et al.*, 2021) statistic utilizing our data set of 792 923 high-quality SNPs. The ABBA–BABA four-population test has been widely utilized across a diverse array of taxa (Durand *et al.*, 2011; Sun *et al.*, 2018; W. Zhang *et al.*, 2018; Sadanandan *et al.*, 2020) to identify a significant excess of shared alleles between two groups over what would be expected from incomplete lineage sorting alone. We found highly significant positive *D* values (indicating signatures of gene flow) between all lineage quartets that are compatible with the species tree (Fig. 3c). Significant signatures of introgression were identified between even the two most highly differentiated lineages, BC and CO. However, it is not possible to determine the amount of introgression between taxon pairs from the ABBA–BABA test alone, as *D* is not an unbiased estimator (Martin *et al.*, 2015). Still, the presence of highly significant *D* values across all lineages, regardless of geographic or phylogenetic distance, implies that introgression events are not rare and isolated occurrences within *B. edulis*. Nonetheless, the role these events are playing in the divergence of *B. edulis* lineages is unclear. Introgression and hybridization have received extensive recent attention as potential drivers of novel phenotypes and genotypes in hybrid populations (Gante *et al.*, 2016; McVay *et al.*, 2017; W. Zhang *et al.*, 2018). However, the role that introgression plays in the breakdown of genomic differentiation between disparate groups is less well known (Abbott *et al.*, 2013). We found that high levels of genomic differentiation are maintained within *B. edulis* despite substantial introgression. Theoretical work has also indicated that differentiation can remain after introgression, although only under low migration demographic conditions (Lindtke & Alex Buerkle, 2015). By contrast, we identified a lack of IBD or subpopulation structure within widely dispersed lineages, suggesting potentially high migration rates. This paradox indicates that forces such as local adaptation may be maintaining reproductive isolation among *B. edulis* lineages in the face of high dispersal capacity.

Identifying the genetic basis of local adaptation in *B. edulis*

Little is known about the selective pressures that contribute to divergence in ectomycorrhizal fungi. However, genome-wide outlier analyses can identify loci carrying signatures of local adaptation, utilizing no *a priori* information on the ecology of the organism. To identify putative adaptive loci contributing to lineage divergence, we performed a genome-wide scan to identify highly divergent genes (mean pairwise F_{ST} and $D_{(xy)}$ in top 5% of each metric) that also contained putative locally adaptive SNPs (identified by PCAdapt) (Fig. 3d). We identified 20 putative outlier genes, of which 8, 5, 3, 3, and 1 gene(s) were most divergent in the EU, BC, WC, CO, and EC lineages, respectively (Table S4). Of these 20 genes, 12 had known predicted functions (Fig. 3d).

Two of the three most significant outliers have been the subject of previous work in other fungal taxa and have functions that align with mechanisms previously proposed to contribute to divergence in ectomycorrhizal fungi. The first outlier locus, EDU-000167, which is divergent in the CO lineage, is predicted to produce a pyridoxal phosphate-dependent transferase (IPR015421). A recent study found that the pyridoxal-5′-phosphate-dependent transferase is involved in the production of indole alkaloids in *Curvularia* (Dai *et al.*, 2020). Ectomycorrhizal indole alkaloids, specifically hypaphorine, were the first fungal molecules identified that regulate host symbiosis-related genes during the colonization process and may be involved in host

specificity (Béguiristain & Lapeyrie, 1997; Ditengou *et al.*, 2000; Veličkovic' *et al.*, 2019). Moreover, this function was identified in *Pisolithus tinctorius*, a taxon within the same order as *B. edulis* (Boletales). Shifts in host specificity are thought to be a primary driver of divergence in ectomycorrhizal fungi (Bruns, 2002). In addition, they have been shown to evolve rapidly, leading to numerous patterns of compatible and incompatible host associations within a single ectomycorrhizal genus (den Bakker *et al.*, 2004; Tedersoo *et al.*, 2009; Liao *et al.*, 2016; Mujic *et al.*, 2019) and can lead to dynamic changes in genome evolution (Lofgren *et al.*, 2021). Regardless, divergence within loci involved in the complex chemical handshake between ectomycorrhizae and host can likely lead to reproductive barriers, facilitating lineage divergence. *B. edulis* is well known to colonize a diverse array of hosts in Europe (Águeda *et al.*, 2008; Beugelsdijk *et al.*, 2008; Dentinger *et al.*, 2010). However, it is thought to rarely occur without gymnosperm hosts in North America (Smith, 2005). If divergence in the gene EDU-000167 is driving, or indicative of, shifts in host preference in the CO lineage, this would provide one explanation for the limited admixture and high divergence of CO, despite geographic and phylogenetic proximity to the WC lineage.

The second putative outlier locus, EDU-010436, which is divergent in BC, was predicted to have aspartic protease activity (GO: 0004190, IPR013320) and contained a predicted secretion signal, suggesting that it has an extracellular function. Aspartic proteases have been shown to be the primary component of extracellular protease activity in numerous ectomycorrhizal taxa (Shah *et al.*, 2013) and are well known to be intricately involved in litter degradation (Bending & Read, 1995). In addition, EDU-010436 exhibited the lowest nucleotide diversity (π) of the three outliers ($\pi = 0.0061$), which is well within the lowest 3% of all genes, providing strong evidence that it is currently under selection in the BC lineage. Recent work indicates that most ectomycorrhizal fungi retain some capacity to decompose organic material and actively acquire carbon and nitrogen from decomposition (Vaario *et al.*, 2012; Talbot *et al.*, 2013; Bödeker *et al.*, 2016; Martin *et al.*, 2016; Akroume *et al.*, 2018; Miyauchi *et al.*, 2020). Moreover, saprotrophic capacity and the conditions under which saprotrophic activity is conducted differ between closely related taxa, suggesting a potential difference in selective pressures along the mutualist to facultative-saprotroph spectrum (Lindahl & Tunlid, 2015). If selection in EDU-010436 indicates some shift in saprotrophicity in the BC lineage, this could have created an ecological reproductive barrier where hybrids experience reduced fitness as they exhibit an intermediate saprotrophic phenotype. In addition, the coast of British Columbia, where the BC lineage is predominately distributed, is well known for high levels of precipitation and moderate seasonal temperatures, which may allow for high decomposition rates and large pools of readily accessible carbon and nitrogen (Talbot & Treseder, 2010), hypothetically relaxing the purifying selection that would maintain saprotrophic capacity in the BC lineage. However, even for this well-characterized outlier, it is unknown whether it serves the same purpose in *B. edulis* or whether it might have been co-opted for a novel function, necessitating further research. Regardless, genomic outlier analysis indicates that divergent loci are putatively involved in adaptation to local environmental conditions, lending further evidence to the role of local adaptation in maintaining lineage differentiation.

Identifying climatic partitioning within *B. edulis*

Due to limited knowledge about the forces that structure ectomycorrhizal niches, it is unknown whether the strong geographic structure seen in *B. edulis* could be due to strong selection for adaptation to local environmental conditions. Moreover, there is little *a priori* knowledge of the capacity for lineages of *B. edulis* to occupy unique climatic or ecological niches, capacities that may help to explain the observed pattern of strong genomic divergence despite introgression. To overcome this limitation, we used ecological niche modeling (Phillips *et al.*, 2006) to create models of geographic environmental suitability based on the 19 Bioclim variables (Table S3), calculated niche overlap, and assessed whether the lineages occupy discrete climatic niches.

As expected given the strong geographic structure of *B. edulis* lineages, ecological niche models identified low-to-moderate levels of niche overlap between lineages (Table S2) and relatively limited distribution overlap (Fig. 4 right). Even within North America, where there is currently geographic overlap between several lineages, niche models suggest that the samples we analyzed may lie at the edge of their potential distributions. However, the ecological niche model for the AK lineage indicates an expansive range of environmental suitability, stretching from Eastern Europe to the east coast of North America, and greatly overlapping in distribution with the EU and EC lineages. The AK lineage also has the highest level of admixture, predominately with the EU and EC lineages, suggesting that niche overlap may result in increased gene flow. Across all models, Bioclim 8 (Mean Temperature of Wettest Quarter) explained the most variation, followed by Bioclim 3 (Isothermality) and Bioclim 6 (Min Temperature of Coldest Month) (Fig. S10). Overall, niche modeling suggests that all lineages other than AK have limited geographic and niche overlap, potentially indicating the occupation of unique climatic niche spaces and further reinforcing the potential role of local adaptation in maintaining lineage fidelity in the face of high dispersal capacity.

Demographic and paleo-climatic niche modeling to identify correlations between isolation and genome-wide divergence

Separation during glacial maxima is known to contribute to the differentiation of populations through the reduction in homogenizing gene flow, allowing genomic incompatibilities to accumulate and prezygotic reproductive barriers to form (Weir & Schluter, 2004; April *et al.*, 2013; Roberts & Hamann, 2015). While we hypothesize that local adaptation is the primary driving force behind the pattern of divergence found in *B. edulis*, periods of allopatric isolation due to glaciation cycles can create similar patterns of geographic structure with limited local adaptation. To investigate the relative importance of local adaptation versus

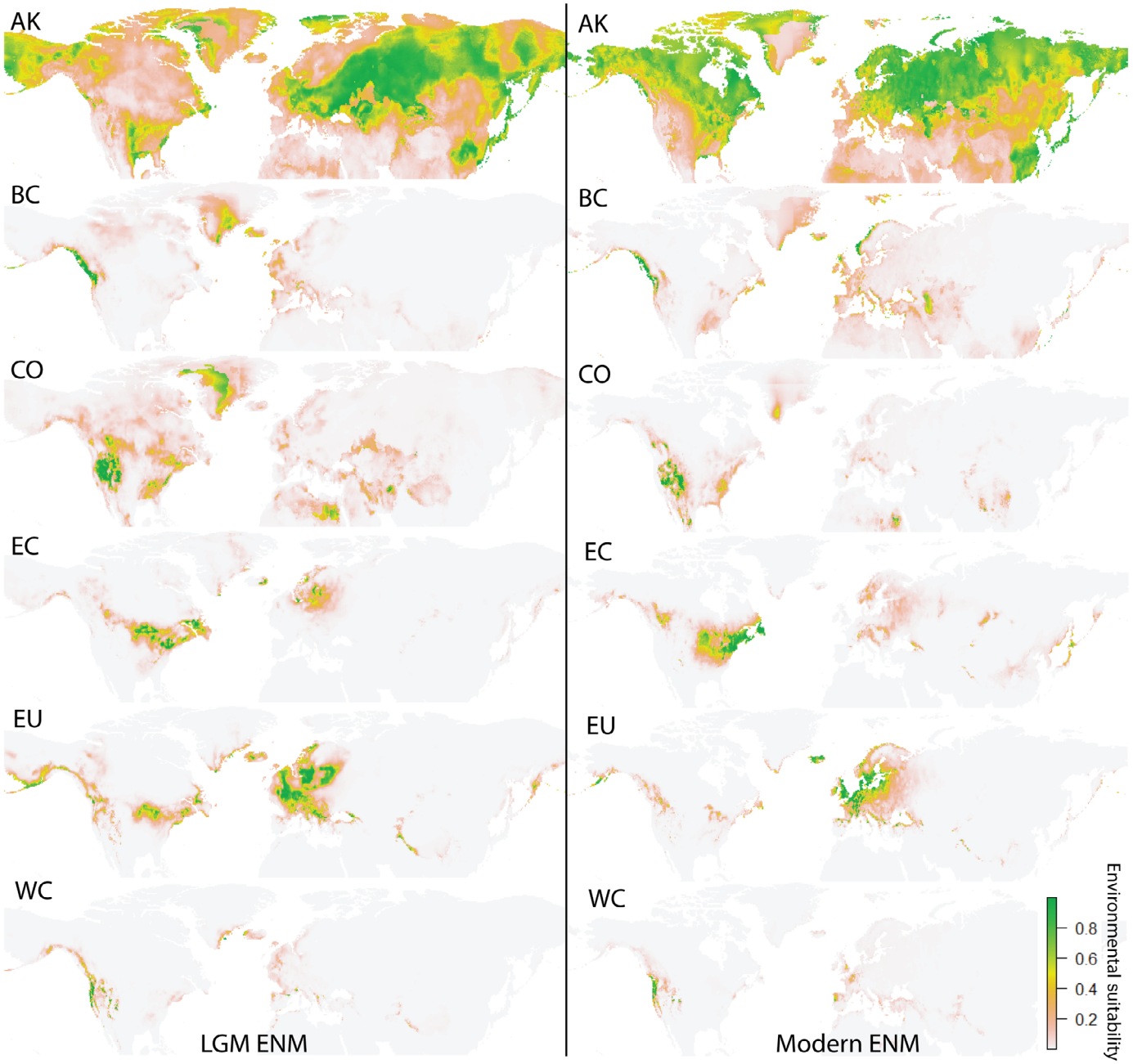

Fig. 4 Suitability distribution of *Boletus edulis* populations determined by ecological niche modeling (ENM) using the 19 Bioclim variables modeled during the last glacial maximum (LGM) 22 ka (thousand years ago; left) and empirical values measured from 1950 to 2000 (right). Regions in green indicate areas with high likelihood of environmental suitability. AK, Alaska/Russia; BC, British Columbia; CO, Colorado; EC, east coast North America; EU, Europe; WC, west coast North America.

allopatric isolation to population divergence, we again used ecological niche modeling to identify the potential geographic distributions of lineages during the last glacial maximum (LGM *c.* 22 000 years ago). We then calculated niche overlap (Warren *et al.*, 2008) to identify lineages that potentially shared refugia and calculated the change in niche overlap between lineage pairs from the LGM to the current day to identify whether these lineages are presently experiencing more or less potential contact than during the LGM.

Ecological niche modeling of *B. edulis* lineages during the LGM found that, on average, niche overlap was greater (mean = 0.426) during the LGM than the amount of contemporary overlap (mean = 0.397). However, the impact of the LGM climate on niche overlap varied widely between lineage pairs (Table S2). For example, niche overlap between the AK/EC lineages increased from the LGM to the current day and a clear break in population connectivity throughout Canada can be seen in the AK lineage. This pattern is consistent with the presence of

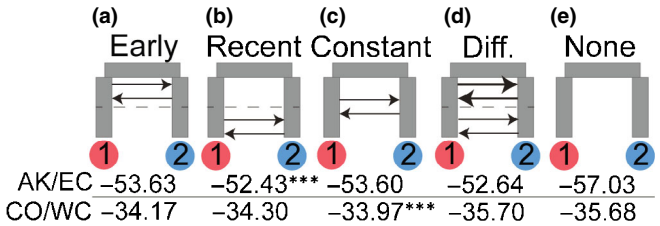

Fig. 5 Representations of the five demographic models tested using two pairs of sister lineages (AK/EC and CO/WC). From left to right, (a) gene flow after lineage divergence with subsequent loss of connectivity, (b) secondary contact with an initial period of isolation, (c) constant gene flow since split, (d) differential gene flow with high initial gene flow and then the accumulation of reproductive barriers, (e) and no gene flow after divergence. Values are mean likelihood values across 100 replicates. '***' indicates significance for the highest likelihood values ($P < 0.00001$). The recent gene flow and constant gene flow models had the highest likelihood for the AK/EC and CO/WC lineages, respectively.

large glacial ice sheets known to have persisted across this region during the LGM (Webb & Bartlein, 1992). By contrast, niche overlap between the CO and WC lineages decreased slightly from the LGM to the current day, presumably due to an increase in low-elevation habitat availability due to lower LGM temperatures in North America (Webb & Bartlein, 1992), a pattern that has also been found in numerous tree taxa, including putative ectomycorrhizal hosts (Roberts & Hamann, 2015). Overall, there appear to be contrasting signatures of isolation during the LGM, where most lineage pairs experienced no change to moderate gain of potential population connectivity (CO/WC), while a few lineages exhibited a substantial reduction in connectivity (AK/EC).

Ecological niche modeling does not empirically test whether populations with niche overlap experience migration during periods of contact or isolation. To identify whether pairs of lineages indeed experienced periods of isolation with limited gene flow, we used coalescent simulations to model five demographic scenarios, focusing on two pairs of sister lineages, AK/EC and WC/CO, with contrasting glaciation dynamics (Fig. 5). Coalescence demographic modeling found the best support for a secondary contact model (Fig. 5b) between the AK/EC lineages where AK/EC most likely experienced a period of postdivergence isolation and are now experiencing gene flow following their reintroduction via postglacial migration. By contrast, the demographic model with the highest likelihood for WC/CO was a constant gene flow model with no period of isolation (Fig. 5c). These results corroborate the ecological niche modeling results, which suggest that connectivity between AK/EC was highly reduced or cut off during the LGM, while WC/CO experienced little to no change in connectivity between the LGM and modern day. Despite the strong evidence for periods of isolation during glacial maxima, the AK/EC pair exhibit the least population differentiation and genic divergence and have the strongest signatures of contemporary gene flow of all lineages. This is in stark contrast to the WC/CO lineages, which show no evidence for true isolation yet maintain strong genome-wide differentiation. Moreover, at the lowest end of the proposed range of divergence times between AK/EC (720 ka), these lineages will have experienced eight major glaciation cycles (Augustin *et al.*, 2004), indicating that gene flow can be resumed after multiple recurrent periods of isolation acting over almost a million years. This suggests that allopatric isolation is not a necessary step in the process of divergence and that differentiation can be initiated despite connectivity between groups.

Conclusions

The contributions of demography, introgression, and adaptation to the origin and shaping of lineage divergence are poorly understood. Here, we identified six lineages within the globally distributed *B. edulis* that exhibit strong geographic structure and moderate-to-high levels of genome-wide divergence. Within these lineages, we found that periods of allopatric isolation are not greatly contributing to genomic divergence. Lineages that have likely experienced numerous cycles of true isolation that should allow for genomic incompatibilities to form have significantly lower levels of divergence and strong signatures of ongoing gene flow. By contrast, lineages that likely have not experienced allopatric isolation possess far greater levels of genomic differentiation. In *Fungi*, it has been suggested that true prezygotic reproductive isolation due to genomic incompatibilities rarely develops (Gladieux *et al.*, 2014). For example, introgression has been identified between highly diverged groups across a diverse array of fungal taxa (Kauserud *et al.*, 2007; Jargeat *et al.*, 2010; Montarry *et al.*, 2010; Stukenbrock *et al.*, 2012), indicating that long-separated groups can hybridize. As a consequence, this places a greater emphasis on the role of other mechanisms that can generate reproductive barriers, such as local adaptation, in the speciation process. Our study provides further evidence for the importance of local adaptation and divergent selection mediated by prevailing ecological conditions, rather than prezygotic barriers such as allopatry or genomic incompatibility, in the role of population divergence in *Fungi*.

Acknowledgements

The authors are grateful to the many institutions and individuals who provided the specimens used in this study. The authors would also like to thank Karrin Tenant for her work in the laboratory. This work was supported by NSF-DEB award #2114785.

Competing interests

None declared.

Author contributions

KT designed the study, performed laboratory protocols, conducted bioinformatic and statistical analyses, and wrote the manuscript. JIH provided technical expertise and collaborated on writing the manuscript. BTMD worked on study design, specimen and funding acquisition, and collaborated on writing the manuscript.

ORCID

Bryn T. M. Dentinger https://orcid.org/0000-0001-7965-4389
J. I. Hoffman https://orcid.org/0000-0001-5895-8949
Keaton Tremble https://orcid.org/0000-0002-0788-2830

Data availability

All short-read genome sequences and the newly created *B. edulis* reference genome are publicly available on the Short Read Archive and GenBank under the accession no. JAIQWV000000000.

References

Abbott R, Albach D, Ansell S, Arntzen JW, Baird SJE, Bierne N, Boughman J, Brelsford A, Buerkle CA, Buggs R *et al.* 2013. Hybridization and speciation. *Journal of Evolutionary Biology* **26**: 229–246.

Águeda B, Parladé J, Fernández-Toirán LM, Cisneros Ó, de Miguel AM, Modrego MP, Martínez-Peña F, Pera J. 2008. Mycorrhizal synthesis between *Boletus edulis* species complex and rockroses (*Cistus* sp.). *Mycorrhiza* **18**: 443–449.

Akroume E, Maillard F, Bach C, Hossann C, Brechet C, Angeli N, Zeller B, Saint-André L, Buée M. 2018. First evidences that the ectomycorrhizal fungus *Paxillus involutus* mobilizes nitrogen and carbon from saprotrophic fungus necromass. *Environmental Microbiology* **21**: 197–208.

Almagro Armenteros JJ, Tsirigos KD, Sønderby CK, Petersen TN, Winther O, Brunak S, von Heijne G, Nielsen H. 2019. SignalP 5.0 improves signal peptide predictions using deep neural networks. *Nature Biotechnology* **37**: 420–423.

April J, Hanner RH, Dion-Côté A-M, Bernatchez L. 2013. Glacial cycles as an allopatric speciation pump in north-eastern American freshwater fishes. *Molecular Ecology* **22**: 409–422.

Arora D, Frank J. 2014. *Boletus rubriceps*, a new species of porcini from the southwestern USA. *North American Fungi* **9**: 1–11.

Arora D. 2008. California Porcini: three new taxa, observations on their harvest, and the tragedy of no commons. *Economic Botany* **62**: 356–375.

Augustin L, Barbante C, Barnes PR, Barnola JM, Bigler M, Castellano E, Cattani O, Chappellaz J, Dahl-Jensen D, Delmonte B *et al.* 2004. Eight glacial cycles from an Antarctic ice core. *Nature* **429**: 623–628.

den Bakker HC, Zuccarello GC, Kuyper THW, Noordeloos ME. 2004. Evolution and host specificity in the ectomycorrhizal genus *Leccinum*. *New Phytologist* **163**: 201–215.

Bankevich A, Nurk S, Antipov D, Gurevich AA, Dvorkin M, Kulikov AS, Lesin VM, Nikolenko SI, Pham S, Prjibelski AD *et al.* 2012. SPAdes: a new genome assembly algorithm and its applications to single-cell sequencing. *Journal of Computational Biology* **19**: 455–477.

Béguiristain T, Lapeyrie F. 1997. Host plant stimulates hypaphorine accumulation in *Pisolithus tinctorius* hyphae during ectomycorrhizal infection while excreted fungal hypaphorine controls root hair development. *New Phytologist* **136**: 525–532.

Bending GD, Read DJ. 1995. The structure and function of the vegetative mycelium of ectomycorrhizal plants. VI. Activities of nutrient mobilizing enzymes in birch litter colonized by *Paxillus involutus* (Fr.) Fr. *New Phytologist* **130**: 411–417.

Beugelsdijk DCM, van der Linde S, Zuccarello GC, den Bakker HC, Draisma SGA, Noordeloos ME. 2008. A phylogenetic study of *Boletus* section *Boletus* in Europe. *Persoonia – Molecular Phylogeny and Evolution of Fungi* **20**: 1–7.

Bierne N, Gagnaire P-A, David P. 2013. The geography of introgression in a patchy environment and the thorn in the side of ecological speciation. *Current Zoology* **59**: 72–86.

Bödeker ITM, Lindahl BD, Olson Å, Clemmensen KE. 2016. Mycorrhizal and saprotrophic fungal guilds compete for the same organic substrates but affect decomposition differently. *Functional Ecology* **30**: 1967–1978.

Bohonak AJ. 1999. Dispersal, gene flow, and population structure. *The Quarterly Review of Biology* **74**: 21–45.

Bouckaert RR, Drummond AJ. 2017. bModelTest: Bayesian phylogenetic site model averaging and model comparison. *BMC Evolutionary Biology* **17**: 42.

Bragason Á. 1995. Exotic trees in Iceland. *Búvísindi* **9**: 37–45.

Branco S, Bi K, Liao HL, Gladieux P, Badouin H, Ellison CE, Nguyen NH, Vilgalys R, Peay KG, Taylor JW *et al.* 2017. Continental-level population differentiation and environmental adaptation in the mushroom *Suillus brevipes*. *Molecular Ecology* **26**: 2063–2076.

Bruns TD. 2002. Host specificity in ectomycorrhizal communities: what do the exceptions tell us? *Integrative and Comparative Biology* **42**: 352–359.

Callahan CM, Rowe CA, Ryel RJ, Shaw JD, Madritch MD, Mock KE. 2013. Continental-scale assessment of genetic diversity and population structure in quaking aspen (*Populus tremuloides*). *Journal of Biogeography* **40**: 1780–1791.

Cantalapiedra CP, Hernández-Plaza A, Letunic I, Bork P, Huerta-Cepas J. 2021. eggNOG-mapper v.2: functional annotation, orthology assignments, and domain prediction at the metagenomic scale. *Molecular Biology and Evolution* **38**: 5825–5829.

Chen J-J, Cui B-K, Zhou L-W, Korhonen K, Dai Y-C. 2015. Phylogeny, divergence time estimation, and biogeography of the genus *Heterobasidion* (Basidiomycota, Russulales). *Fungal Diversity* **71**: 185–200.

Chen S, Zhou Y, Chen Y, Gu J. 2018. fastp: an ultra-fast all-in-one Fastq preprocessor. *Bioinformatics* **34**: i884–i890.

Coyne JA, Coyne HA, Allen Orr H. 2004. *Speciation*. Oxford, UK: Oxford University Press.

Dai GZ, Han WB, Mei YN, Xu K, Jiao RH, Ge HM, Tan RX. 2020. Pyridoxal-5′-phosphate–dependent bifunctional enzyme cat-alyzed biosynthesis of indolizidine alkaloids in fungi. *Proceedings of the National Academy of Sciences, USA* **117**: 1174–1180.

Danecek P, Auton A, Abecasis G, Albers CA, Banks E, DePristo MA, Handsaker RE, Lunter G, Marth GT, Sherry ST *et al.* 2011. The variant call format and VCFtools. *Bioinformatics* **27**: 2156–2158.

deMenocal PB. 2004. African climate change and faunal evolution during the Pliocene–Pleistocene. *Earth and Planetary Science Letters* **220**: 3–24.

Dentinger BT, Ammirati JF, Both EE, Desjardin DE, Halling RE, Henkel TW, Moreau PA, Nagasawa E, Soytong K, Taylor AF *et al.* 2010. Molecular phylogenetics of porcini mushrooms (*Boletus* section *Boletus*). *Molecular Phylogenetics and Evolution* **57**: 1276–1292.

Dentinger BTM, Suz LM. 2014. What's for dinner? Undescribed species of porcini in a commercial packet. *PeerJ* **2**: e570.

Ditengou FA, Béguiristain T, Lapeyrie F. 2000. Root hair elongation is inhibited by hypaphorine, the indole alkaloid from the ectomycorrhizal fungus *Pisolithus tinctorius*, and restored by indole-3-acetic acid. *Planta* **211**: 722–728.

Dixo M, Metzger JP, Morgante JS, Zamudio KR. 2009. Habitat fragmentation reduces genetic diversity and connectivity among toad populations in the Brazilian Atlantic Coastal Forest. *Biological Conservation* **142**: 1560–1569.

Durand EY, Patterson N, Reich D, Slatkin M. 2011. Testing for ancient admixture between closely related populations. *Molecular Biology and Evolution* **28**: 2239–2252.

Elith J, Phillips SJ, Hastie T, Dudík M, Chee YE, Yates CJ. 2011. A statistical explanation of MaxEnt for ecologists. *Diversity and Distributions* **17**: 43–57.

Ericson DB, Ewing M, Wollin G. 1963. Pliocene–Pleistocene boundary in deep-sea sediments: extinctions and evolutionary changes in microfossils clearly define the abrupt onset of the Pleistocene. *Science* **139**: 727–737.

Evans LM, Slavov GT, Rodgers-Melnick E, Martin J, Ranjan P, Muchero W, Brunner AM, Schackwitz W, Gunter L, Chen J-G *et al.* 2014. Population genomics of *Populus trichocarpa* identifies signatures of selection and adaptive trait associations. *Nature Genetics* **46**: 1089–1096.

Excoffier L, Marchi N, Marques DA, Matthey-Doret R, Gouy A, Sousa VC. 2021. fastsimcoal2: demographic inference under complex evolutionary scenarios. *Bioinformatics* **37**: 4882–4885.

Ferris KG, Barnett LL, Blackman BK, Willis JH. 2017. The genetic architecture of local adaptation and reproductive isolation in sympatry within the *Mimulus guttatus* species complex. *Molecular Ecology* **26**: 208–224.

Feulner PG, Chain FJ, Panchal M, Huang Y, Eizaguirre C, Kalbe M, Lenz TL, Samonte IE, Stoll M, Bornberg-Bauer E *et al.* 2015. Genomics of divergence

along a continuum of parapatric population differentiation. *PLoS Genetics* **11**: e1004966.

Fick SE, Hijmans RJ. 2017. WorldClim 2: new 1-km spatial resolution climate surfaces for global land areas. *International Journal of Climatology* **37**: 4302–4315.

Fisher RA. 1930. *The genetical theory of natural selection*. Oxford, UK: Clarendon Press.

Frichot E, Mathieu F, Trouillon T, Bouchard G, François O. 2014. Fast and efficient estimation of individual ancestry coefficients. *Genetics* **196**: 973–983.

Gaines MS, Diffendorfer JE, Tamarin RH, Whittam TS. 1997. The effects of habitat fragmentation on the genetic structure of small mammal populations. *Journal of Heredity* **88**: 294–304.

Gante HF, Matschiner M, Malmstrøm M, Jakobsen KS, Jentoft S, Salzburger W. 2016. Genomics of speciation and introgression in Princess cichlid fishes from Lake Tanganyika. *Molecular Ecology* **25**: 6143–6161.

Garcia-Elfring A, Barrett RDH, Combs M, Davies TJ, Munshi-South J, Millien V. 2017. Admixture on the northern front: population genomics of range expansion in the white-footed mouse (*Peromyscus leucopus*) and secondary contact with the deer mouse (*Peromyscus maniculatus*). *Heredity* **119**: 447–458.

Geraldes A, Farzaneh N, Grassa CJ, McKown AD, Guy RD, Mansfield SD, Douglas CJ, Cronk QCB. 2014. Landscape genomics of *Populus trichocarpa*: the role of hybridization, limited gene flow, and natural selection in shaping patterns of population structure. *Evolution* **68**: 3260–3280.

Giraud T, Refrégier G, le Gac M, de Vienne DM, Hood ME. 2008. Speciation in fungi. *Fungal Genetics and Biology* **45**: 791–802.

Gladieux P, Ropars J, Badouin H, Branca A, Aguileta G, Vienne DM, Rodríguez de la Vega RC, Branco S, Giraud T. 2014. Fungal evolutionary genomics provides insight into the mechanisms of adaptive divergence in eukaryotes. *Molecular Ecology* **23**: 753–773.

Grigoriev IV, Nikitin R, Haridas S, Kuo A, Ohm R, Otillar R, Riley R, Salamov A, Zhao X, Korzeniewski F *et al.* 2014. MycoCosm portal: gearing up for 1000 fungal genomes. *Nucleic Acids Research* **42**: D699–D704.

He M-Q, Zhao R-L, Hyde KD, Begerow D, Kemler M, Yurkov A, McKenzie EHC, Raspé O, Kakishima M, Sánchez-Ramírez S *et al.* 2019. Notes, outline and divergence times of Basidiomycota. *Fungal Diversity* **99**: 105–367.

Hickey AJ, Lavery SD, Hannan DA, Baker CS, Clements KD. 2009. New Zealand triplefin fishes (family Tripterygiidae): contrasting population structure and mtDNA diversity within a marine species flock. *Molecular Ecology* **18**: 680–696.

Hoang DT, Chernomor O, von Haeseler A, Minh BQ, Vinh LS. 2018. UFBoot2: improving the ultrafast bootstrap approximation. *Molecular Biology and Evolution* **35**: 518–522.

Hoban S, Kelley JL, Lotterhos KE, Antolin MF, Bradburd G, Lowry DB, Poss ML, Reed LK, Storfer A, Whitlock MC. 2016. Finding the genomic basis of local adaptation: pitfalls, practical solutions, and future directions. *The American Naturalist* **188**: 379–397.

Hoff KJ, Stanke M. 2018. Predicting genes in single genomes with Augustus. *Current Protocols in Bioinformatics* **65**: e57.

Hohenlohe PA, Bassham S, Etter PD, Stiffler N, Johnson EA, Cresko WA. 2010. Population genomics of parallel adaptation in threespine stickleback using sequenced RAD tags. *PLoS Genetics* **6**: e1000862.

Ii W, Cutler D, Bradshaw AJ, Dentinger BTM. 2021. What's for dinner this time?: DNA authentication of "wild mushrooms" in food products sold in the USA. *PeerJ* **9**: e11747.

Jargeat P, Martos F, Carriconde F, Gryta H, Moreau PA, Gardes M. 2010. Phylogenetic species delimitation in ectomycorrhizal fungi and implications for barcoding: the case of the *Tricholoma scalpturatum* complex (Basidiomycota). *Molecular Ecology* **19**: 5216–5230.

Jiang S, Luo M-X, Gao R-H, Zhang W, Yang Y-Z, Li Y-J, Liao P-C. 2019. Isolation-by-environment as a driver of genetic differentiation among populations of the only broad-leaved evergreen shrub *Ammopiptanthus mongolicus* in Asian temperate deserts. *Scientific Reports* **9**: 12008.

Jombart T. 2008. adegenet: a R package for the multivariate analysis of genetic markers. *Bioinformatics* **24**: 1403–1405.

Jones P, Binns D, Chang H-Y, Fraser M, Li W, McAnulla C, McWilliam H, Maslen J, Mitchell A, Nuka G *et al.* 2014. InterProScan 5: genome-scale protein function classification. *Bioinformatics* **30**: 1236–1240.

Kalyaanamoorthy S, Minh BQ, Wong TKF, von Haeseler A, Jermiin LS. 2017. ModelFinder: fast model selection for accurate phylogenetic estimates. *Nature Methods* **14**: 587–589.

Katoh K, Rozewicki J, Kazunori DY. 2017. Mafft online service: multiple sequence alignment, interactive sequence choice and visualization. *Briefings in Bioinformatics* **20**: 1160–1166.

Kauserud H, Svegården IB, Decock C, Hallenberg N. 2007. Hybridization among cryptic species of the cellar fungus *Coniophora puteana* (Basidiomycota). *Molecular Ecology* **16**: 389–399.

Klimo E, Hager H, Kulhavy J, eds. 2000. Spruce monocultures in Central Europe: problems and prospects. *European Forestry Institute Proceedings* no. 33. Joensuu, Finland: European Forest Institute.

Klimova A, Hoffman JI, Gutierrez-Rivera JN, Leon de la Luz J, Ortega-Rubio A. 2017. Molecular genetic analysis of two native desert palm genera, *Washingtonia* and *Brahea*, from the Baja California Peninsula and Guadalupe Island. *Ecology and Evolution* **7**: 4919–4935.

Kohler A, Kuo A, Nagy LG, Morin E, Barry KW, Buscot F, Canbäck B, Choi C, Cichocki N, Clum A *et al.* 2015. Convergent losses of decay mechanisms and rapid turnover of symbiosis genes in mycorrhizal mutualists. *Nature Genetics* **47**: 410–415.

Korunes KL, Samuk K. 2021. pixy: unbiased estimation of nucleotide diversity and divergence in the presence of missing data. *Molecular Ecology Resources* **21**: 1359–1368.

Kryvokhyzha D. 2021. *gatk: the best practice for genotype calling in a non-model organism*. [WWW document] URL https://evodify.com/gatk-in-non-model-organism/ [accessed 7 April 2021].

Langmead B, Salzberg SL. 2012. Fast gapped-read alignment with Bowtie 2. *Nature Methods* **9**: 357–359.

Liao H-L, Chen Y, Vilgalys R. 2016. Metatranscriptomic study of common and host-specific patterns of gene expression between pines and their symbiotic ectomycorrhizal fungi in the genus *Suillus*. *PLoS Genetics* **12**: e1006348.

Lindahl BD, Tunlid A. 2015. Ectomycorrhizal fungi – potential organic matter decomposers, yet not saprotrophs. *New Phytologist* **205**: 1443–1447.

Lindtke D, Alex Buerkle C. 2015. The genetic architecture of hybrid incompatibilities and their effect on barriers to introgression in secondary contact. *Evolution* **69**: 1987–2004.

Lofgren LA, Nguyen NH, Vilgalys R, Ruytinx J, Liao HL, Branco S, Kuo A, LaButti K, Lipzen A, Andreopoulos W *et al.* 2021. Comparative genomics reveals dynamic genome evolution in host specialist ectomycorrhizal fungi. *New Phytologist* **230**: 774–792.

Luu K, Bazin E, Blum MGB. 2017. pcadapt: an R package to perform genome scans for selection based on principal component analysis. *Molecular Ecology Resources* **17**: 67–77.

Malinsky M, Matschiner M, Svardal H. 2021. Dsuite – Fast *D*-statistics and related admixture evidence from Vcf files. *Molecular Ecology Resources* **21**: 584–595.

Marques DA, Jones FC, di Palma F, Kingsley DM, Reimchen TE. 2018. Experimental evidence for rapid genomic adaptation to a new niche in an adaptive radiation. *Nature Ecology & Evolution* **2**: 1128–1138.

Martin F, Kohler A, Murat C, Veneault-Fourrey C, Hibbett DS. 2016. Unearthing the roots of ectomycorrhizal symbioses. *Nature Reviews Microbiology* **14**: 760–773.

Martin SH, Dasmahapatra KK, Nadeau NJ, Salazar C, Walters JR, Simpson F, Blaxter M, Manica A, Mallet J, Jiggins CD. 2013. Genome-wide evidence for speciation with gene flow in Heliconius butterflies. *Genome Research* **23**: 1817–1828.

Martin SH, Davey JW, Jiggins CD. 2015. Evaluating the use of ABBA–BABA statistics to locate introgressed loci. *Molecular Biology and Evolution* **32**: 244–257.

McKown AD, Klápště J, Guy RD, Geraldes A, Porth I, Hannemann J, Friedmann M, Muchero W, Tuskan GA, Ehlting J *et al.* 2014. Genome-wide association implicates numerous genes underlying ecological trait variation in natural populations of *Populus trichocarpa*. *New Phytologist* **203**: 535–553.

McVay JD, Hipp AL, Paul SM. 2017. A genetic legacy of introgression confounds phylogeny and biogeography in oaks. *Proceedings of the Royal Society B: Biological Sciences* **284**: 20170300.

Medema MH, Blin K, Cimermancic P, de Jager V, Zakrzewski P, Fischbach MA, Weber T, Takano E, Breitling R. 2011. antiSMASH: rapid identification, annotation and analysis of secondary metabolite biosynthesis gene clusters in bacterial and fungal genome sequences. *Nucleic Acids Research* **39**: W339–W346.

Merow C, Smith MJ, Silander JA. 2013. A practical guide to MaxEnt for modeling species' distributions: what it does, and why inputs and settings matter. *Ecography* **36**: 1058–1069.

Minh BQ, Schmidt HA, Chernomor O, Schrempf D, Woodhams MD, von Haeseler A, Lanfear R. 2020. IQ-TREE 2: new models and efficient methods for phylogenetic inference in the genomic era. *Molecular Biology and Evolution* **37**: 1530–1534.

Miyauchi S, Kiss E, Kuo A, Drula E, Kohler A, Sánchez-García M, Morin E, Andreopoulos B, Barry KW, Bonito G *et al.* 2020. Large-scale genome sequencing of mycorrhizal fungi provides insights into the early evolution of symbiotic traits. *Nature Communications* **11**: 5125.

Montarry J, Andrivon D, Glais I, Corbiere R, Mialdea G, Delmotte F. 2010. Microsatellite markers reveal two admixed genetic groups and an ongoing displacement within the French population of the invasive plant pathogen *Phytophthora infestans*. *Molecular Ecology* **19**: 1965–1977.

Mujic AB, Huang B, Chen M-J, Wang P-H, Gernandt DS, Hosaka K, Spatafora JW. 2019. Out of western North America: evolution of the Rhizopogon-Pseudotsuga symbiosis inferred by genome-scale sequence typing. *Fungal Ecology* **39**: 12–25.

Nei M. 1987. *Molecular evolutionary genetics*. New York, NY, USA: Columbia University Press.

Nelson CW, Moncla LH, Hughes AL. 2015. SNPGenie: estimating evolutionary parameters to detect natural selection using pooled next-generation sequencing data. *Bioinformatics* **31**: 3709–3711.

Nosil P, Gompert Z, Farkas TE, Comeault AA, Feder JL, Buerkle CA, Parchman TL. 2012. Genomic consequences of multiple speciation processes in a stick insect. *Proceedings of the Royal Society B: Biological Sciences* **279**: 5058–5065.

O'Brien J. 2022. *gdalUtilities: wrappers for 'GDAL' utilities executables*. [WWW document] URL https://github.com/JoshOBrien/gdalUtilities [accessed 30 June 2022].

Ogilvie HA, Bouckaert RR, Drummond AJ. 2017. StarBeast2 brings faster species tree inference and accurate estimates of substitution rates. *Molecular Biology and Evolution* **34**: 2101–2114.

Overcast I. 2022. *easySFS*. [WWW document] URL https://github.com/isaacovercast/easySFS [accessed 30 June 2022].

Palmer J. 2022. *nextgenusfs/funannotate*. [WWW document] URL https://github.com/nextgenusfs/funannotate [accessed 9 November 2022].

Paradis E, Claude J, Stimmer K. 2004. ape: analyses of phylogenetics and evolution in R programming language. *Bioinformatics* **20**: 289–290.

Peñalba JV, Joseph L, Moritz C. 2019. Current geography masks dynamic history of gene flow during speciation in northern Australian birds. *Molecular Ecology* **28**: 630–643.

Pfeifer B, Wittelsbürger U, Ramos-Onsins SE, Lercher MJ. 2014. PopGenome: an efficient swiss army knife for population genomic analyses in R. *Molecular Biology and Evolution* **31**: 1929–1936.

Phillips SJ, Anderson R, Schapire RE. 2006. Maximum entropy modeling of species geographic distributions. *Ecological Modeling* **190**: 231–259.

Purcell S, Neale B, Todd-Brown K, Thomas L, Ferreira MA, Bender D, Maller J, Sklar P, de Bakker PI, Daly MJ *et al.* 2007. Plink: a tool set for whole-genome association and population-based linkage analyses. *The American Journal of Human Genetics* **81**: 559–575.

Puzey JR, Willis JH, Kelly JK. 2017. Population structure and local selection yield high genomic variation in *Mimulus guttatus*. *Molecular Ecology* **26**: 519–535.

Roberts DR, Hamann A. 2015. Glacial refugia and modern genetic diversity of 22 western North American tree species. *Proceedings of the Royal Society B: Biological Sciences* **282**: 20142903.

Rovito SM, Schoville SD. 2017. Testing models of refugial isolation, colonization and population connectivity in two species of montane salamanders. *Heredity* **119**: 265–274.

Sadanandan KR, Low GW, Sridharan S, Gwee CY, Ng EYX, Yuda P, Prawiradilaga DM, Lee JGH, Tritto A, Rheindt FE. 2020. The conservation value of admixed phenotypes in a critically endangered species complex. *Scientific Reports* **10**: 15549.

Seehausen O, Butlin RK, Keller I, Wagner CE, Boughman JW, Hohenlohe PA, Peichel CL, Saetre G-P, Bank C, Brännström Å *et al.* 2014. Genomics and the origin of species. *Nature Reviews Genetics* **15**: 176–192.

Shackleton NJ, Opdyke ND. 1977. Oxygen isotope and palaeomagnetic evidence for early Northern Hemisphere glaciation. *Nature* **270**: 216–219.

Shah F, Rineau F, Canbäck B, Johansson T, Tunlid A. 2013. The molecular components of the extracellular protein-degradation pathways of the ectomycorrhizal fungus *Paxillus involutus*. *New Phytologist* **200**: 875–887.

Siry JP, Cubbage FW, Ahmed MR. 2005. Sustainable forest management: global trends and opportunities. *Forest Policy and Economics* **7**: 551–561.

Sitta N, Floriani M. 2008. Nationalization and globalization trends in the wild mushroom commerce of Italy with emphasis on Porcini (*Boletus edulis* and allied species). *Economic Botany* **62**: 307.

Slater GC, Birney E. 2005. Automated generation of heuristics for biological sequence comparison. *BMC Bioinformatics* **6**: 31.

Smith AH. 2005. In: Smith AH, Thiers HD, eds. *The boletes of Michigan*. Ann Arbor, MI, USA: University of Michigan Press.

Stukenbrock EH, Christiansen FB, Hansen TT, Dutheil JY, Schierup MH. 2012. Fusion of two divergent fungal individuals led to the recent emergence of a unique widespread pathogen species. *Proceedings of the National Academy of Sciences, USA* **109**: 10954–10959.

Sun Y, Abbott RJ, Lu Z, Mao K, Zhang L, Wang X, Ru D, Liu J. 2018. Reticulate evolution within a spruce (*Picea*) species complex revealed by population genomic analysis. *Evolution* **72**: 2669–2681.

Talbot JM, Bruns TD, Smith DP, Branco S, Glassman SI, Erlandson S, Vilgalys R, Peay KG. 2013. Independent roles of ectomycorrhizal and saprotrophic communities in soil organic matter decomposition. *Soil Biology and Biochemistry* **57**: 282–291.

Talbot JM, Treseder KK. 2010. Controls over mycorrhizal uptake of organic nitrogen. *Pedobiologia* **53**: 169–179.

Tedersoo L, Suvi T, Jairus T, Ostonen I, Põlme S. 2009. Revisiting ectomycorrhizal fungi of the genus Alnus: differential host specificity, diversity and determinants of the fungal community. *New Phytologist* **182**: 727–735.

Theodosius D, Foreword by Stephen Jay. 1982. *Genetics and the origin of species: Columbia classics edition*. New York, NY, USA: Columbia University Press.

Tremble K, Suz LM, Dentinger BTM. 2020. Lost in translation: population genomics and long-read sequencing reveals relaxation of concerted evolution of the ribosomal DNA cistron. *Molecular Phylogenetics and Evolution* **148**: 106804.

Twyford AD, Wong ELY, Friedman J. 2020. Multi-level patterns of genetic structure and isolation by distance in the widespread plant *Mimulus guttatus*. *Heredity* **125**: 227–239.

Vaario LM, Heinonsalo J, Spetz P, Pennanen T, Heinonen J, Tervahauta A, Fritze H. 2012. The ectomycorrhizal fungus *Tricholoma matsutake* is a facultative saprotroph *in vitro*. *Mycorrhiza* **22**: 409–418.

Vallejo-Marín M, Friedman J, Twyford AD, Lepais O, Ickert-Bond SM, Streisfeld MA, Yant L, van Kleunen M, Rotter MC, Puzey JR. 2021. Population genomic and historical analysis suggests a global invasion by bridgehead processes in *Mimulus guttatus*. *Communications Biology* **4**: 1–12.

Veličkovic' D, Liao HL, Vilgalys R, Chu R. 2019. Spatiotemporal transformation in the alkaloid profile of Pinus roots in response to mycorrhization. *Journal of Natural Products* **82**: 1382–1386.

Wang IJ. 2013. Examining the full effects of landscape heterogeneity on spatial genetic variation: a multiple matrix regression approach for quantifying geographic and ecological isolation. *Evolution* **67**: 3403–3411.

Wang QB, Yao Y-J. 2005. *Boletus reticuloceps*, a new combination for *Aureoboletus reticuloceps*. *Sydowia* **57**: 131–136.

Warren DL, Glor RE, Turelli M. 2008. Environmental niche equivalency versus conservatism: quantitative approaches to niche evolution. *Evolution* **62**: 2868–2883.

Webb T, Bartlein PJ. 1992. Global changes during the last 3 million years: climatic controls and biotic responses. *Annual Review of Ecology and Systematics* **23**: 141–173.

Weir JT, Schluter D. 2004. Ice sheets promote speciation in boreal birds. *Proceedings of the Royal Society of London. Series B: Biological Sciences* **271**: 1881–1887.

Zhang C, Rabiee M, Sayyari E, Mirarab S. 2018. ASTRAL-III: polynomial time species tree reconstruction from partially resolved gene trees. *BMC Bioinformatics* **19**: 1471–2105.

Zhang H, Yohe T, Huang L, Entwistle S, Wu P, Yang Z, Busk PK, Xu Y, Yin Y. 2018. dbCAN2: a meta server for automated carbohydrate-active enzyme annotation. *Nucleic Acids Research* **46**: W95–W101.

Zhang W, Zhang X, Li K, Wang C, Cai L, Zhuang W, Xiang M, Liu X. 2018. Introgression and gene family contraction drive the evolution of lifestyle and host shifts of hypocrealean fungi. *Mycology* **9**: 176–188.

Zheng Y, Janke A. 2018. Gene flow analysis method, the *D*-statistic, is robust in a wide parameter space. *BMC Bioinformatics* **19**: 10.

Zhong L, Liu H, Ru D, Hu H, Hu Q. 2019. Population genomic evidence for radiative divergence of four Orychophragmus (Brassicaceae) species in eastern Asia. *Botanical Journal of the Linnean Society* **191**: 18–29.

Supporting Information

Additional Supporting Information may be found online in the Supporting Information section at the end of the article.

Fig. S1 Flowchart of population genomic methods and SNP datasets used for each analysis.

Fig. S2 Results of genome-wide outlier analysis.

Fig. S3 Concatenated supermatrix phylogenomic analysis of *Boletus edulis*.

Fig. S4 Population structure of *Boletus edulis* assessed with PCA and neighbor-joining trees.

Fig. S5 Stacked admixture analysis of *Boletus edulis* for $K = 4$–8.

Fig. S6 Within-lineage population structure of the six *Boletus edulis* lineages.

Fig. S7 Divergence date estimation using StarBeast2.

Fig. S8 Whole-genome Tajima's *D* and pairwise genic F_{ST} estimation.

Fig. S9 *QQ* plot analysis of pairwise F_{ST} estimation in *Boletus edulis*.

Fig. S10 Environmental correlation analysis of *Boletus edulis* utilizing 19 Bioclim values.

Fig. S11 Maxent jackknife contributions of Bioclim variables to AUC of AK lineage.

Fig. S12 Maxent jackknife contributions of Bioclim variables to AUC of BC lineage.

Fig. S13 Maxent jackknife contributions of Bioclim variables to AUC of CO lineage.

Fig. S14 Maxent jackknife contributions of Bioclim variables to AUC of EC lineage.

Fig. S15 Maxent jackknife contributions of Bioclim variables to AUC of EU lineage.

Fig. S16 Maxent jackknife contributions of Bioclim variables to AUC of WC lineage.

Table S1 Specimen collection and voucher information.

Table S2 Pairwise population analyses of *Boletus edulis* lineages.

Table S3 19 Bioclim variables for all specimens included in the study.

Table S4 Results from outlier loci analysis and putative function of outlier loci.

Please note: Wiley is not responsible for the content or functionality of any Supporting Information supplied by the authors. Any queries (other than missing material) should be directed to the *New Phytologist* Central Office.